CONCRETE LIBRARY OF JSCE NO. 15, JULY 1990

A Study on the Cracks in RC Deck Slabs of Steel Highway Bridges and the Effectiveness of Expansive Concrete in Preventing Such Cracks

(Translation from Concrete Journal, JCI, Vol.27, No.9, September 1989)



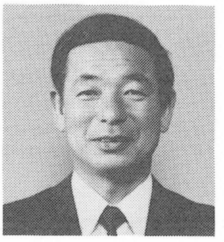
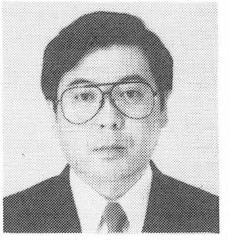

Toshiyasu TOYOFUKU   Iwao NISHIDA   Eizo FUJITA   Kokichi TERAI

SYNOPSIS

In October 1980, expansive concrete was used in the reinforced concrete (hereafter RC) deck slab of the Kuroishihama Bridge (simple steel composite girder) on Nagasaki Expressway as the first attempt of RC deck slabs of steel bridges in Japan. And in June 1982 expansive concrete was also placed in some parts of the Tarami Bridge (4-span continuous steel non-composite plate girder) on Nagasaki Expressway as well. Various follow-up investigations were subsequently carried out at these bridges.
This study reviews the initial cracking mechanism of RC deck slabs based on the follow-up investigations. Also, the study reviews the method of analyzing flexural cracks at the serviceability limit state so that the effectiveness of expansive concrete in preventing cracks can be reflected in the bridge design.

T. TOYOFUKU is an adviser to director at Engineering Department of Osaka Operation Bureau of NIHON DORO KODAN (Japan Highway Public Corporation). He received his Doctor of Engineering Degree from the University of Tokyo in 1988. His research interests are quality control for construction pfoject, maintenance and cotrol of structures and durability of concrete. He is a member of JSCE and JCI.

I. NISHIDA is a professional engineer at Engineering Department of Tokyo First Operation Bureau of NIHON DORO KODAN. At present, he researches superannuative countermeasures (mainly, slab thickness increment and fatigue yield strength of steel member) of reinforced concrete deck slabs and steel bridges on Tomei Expressway constructed twenty years ago. He is a member of JSCE.

E. FUJITA is a deputy-head at Experiment Section of Amagi Construction Office of Fukuoka Construction Bureau of NIHON DORO KODAN. He is in charge of the technology of construction and maintenance on highway.

K. TERAI is belonging to Nippon Engineering Consultants CO., LTD, TOKYO, Japan. He received his Bachelor of Science in Civil Engineering from Shinshyu University in 1972. He is interested in loading capacity and durability of bridges. He is a member of JCI.

---

1. INTRODUCTION

Owing to the fact that a large number of steel highway bridges showed damage to their RC deck slabs, it became important, from the standpoint of bridge design and maintenance, to discover the causes of crack formation and to develop methods for preventing such cracks. Various investigations and studies were conducted over the past decade in an attempt to resolve this problem [1]. Studies on the causes of crack formation have been carried out most notably by Okada et al. [2], [3], Sonoda et al. [4], and Matsui et al. [5], and at the Laboratory of NIHON DORO KODAN (Japan Highway Public Corporation, hereafter KODAN) [6], [7]. A number of countermeasures has also been proposed, including the use of expansive concrete deck slabs. On the design and application of expansive concrete deck slabs Recomended Practice for Expansive Cement Concrete was established by the Japan Society of Civil Engineers (JSCE) [8], and a basic theory, the validity of which was later confirmed through model tests, was formulated by Tsuji and Okamura [9].

The Laboratory of KODAN implemented a two-pronged study from fiscal 1976 to 1985 in which laboratory tests using a large-scale fatigue machine were conducted on one hand and field investigations (load response measurement, damage examination, etc.) on actual bridges were carried out on the other. Through these tests and investigations KODAN was able to arrive at the cause of damage to RC deck slabs. In other words, adverse casting conditions, thermal stress, drying shrinkage stress, and other factors resulted in the development of initial cracks, which progressively enlargened due to the passage of motor vehicle (live loads) and the seepage of rainwater from the top surface of the deck slabs, eventually leading to full-scale damadge.

Based on the above findings, it was believed that the use of expansive concrete would be an effective means of reducing crack formation and preventing full-scale damage to RC deck slabs [10]. Therefore, in October 1980, KODAN used expansive concrete deck slabs in the Kuroishihama Bridge (simple steel composite girder) on Nagasaki Expressway as the first attempt of RC deck slabs of steel bridges in Japan [11], [13]. Furthermore, in June 1982, expansive concrete was again placed in certain sections of the Tarami Bridge (4-span continuous steel non-composite plate girder) on Nagasaki Expressway. Various follow-up investigation subsequently carried out at these bridges [12]～[14].

This study reviews the initial cracking mechanism of RC deck slabs, an area that has not been resolved so far, based on the results of the follow-up investigation. At the same time, the study reviews the method of analyzing flexural cracks at the serviceability limit state in order that the effectiveness of expansive concrete in preventing cracks can be reflected in the bridge design.

It should be noted that the use of expansive concrete deck slabs has been continued by KODAN in Kosuge Overpass (3-span continuous steel non-composite box girder and 2-span continuous steel non-composite plate girder; concrete placed in October 1983) on East Kanto Expressway, Kurinokigawa Bridge (3-span continuous steel struss; concrete placed in October 1984) on Kanetsu Expressway, and Maruki Bridge (4-span continuous steel non-composite plate girder; concrete placed in August 1985) on Tohoku Expressway. Follow-up investigation at these bridges are currently being carried out [15]～[17].

2. OUTLINE OF SURVEYED BRIDGES

Concerning the mix proportion of expansive concrete, unit expansive admixture content of 35 kg/m^3 was determined to give the maximum expansion rate at which compressive strength (unrestrained specimen) does not decline, on the basis of preliminary tests [11], [14]. The expansion rate is $280 \sim 300 \times 10^{-6}$, which corresponds to the chemically prestressed concrete prescribed in the Recommended Practice [9].

An outline of the Kuroishihama Bridge and that of the Suzumekura Bridge (ordinary concrete deck slabs), to which the former was compared, are given in Fig. 1 and Table 1. Table 2 shows the quality of placed concrete. At both bridges, strain was measured up to an age of one year and 11 months and cracking up to an age of seven years. Cracking was measured at four points: between inside girders over a support, between inside girders at a point one-fourth along the span, between inside girders at the central point of the span, and between the inside and outside girders at the same point. Measurement data were divided into the haunch section and the central portion between girders, which excludes the haunch section, and cracking density were calculated by the crack length or the grid density method [18].

An outline of the investigations conducted at the Tarami Bridge is shown in Fig. 2 (also refer to Tables 1 and 2). Since the left and right sides of the bridge are symmetrical to each other, expansive concrete deck slabs were used on the side span of the down side bridge only in order to compare results with the another side. Cracks, strains, temperatures, and internal humidities were investigated up to an age of five years and six months.

Expansive concrete was placed in the morning of June 25, 1982, and ordinary concrete in the afternoon. Placement was subsequently continued in units of four blocks. After five days of adequate moist curing, formwork and shoring were removed on July 14 and 15. Surface paving was then carried out with asphalt. Dummy slabs were constructed in a manner that replicated the conditions for deck slabs.

Cracks were measured at points that are restrained by sway bracing (cross sections A-A, A'-A', and A"-A"), points that are not restrained by sway bracing (cross sections B-B and B'-B'), and over the central support (cross section C-C) for a total of 14 points. Strains were measured at all the above points except cross section A"-A". As shown in Fig. 2(c), this was carried out by installing reinforcing bar gauges and concrete strain gauges.

Temperature readings were obtained from the insides of deck slabs and on the surfaces of girders in cross section A-A. Internal humidity readings were obtained from the expansive concrete section (near cross section A-A) and from the ordinary concrete section (near cross section A'-A'). This was done by drilling 9 mmholes at fixed points (see Fig. 2(d)) on the deck slab bottom and keeping the holes sealed with rubber plugs until the time of reading. To take a reading, a sensitive hygrometer was inserted into a hole and taken out after approximately 20 minutes of sealing.

3. INVESTIGATION RESULTS

3.1 Cracks

Fig. 3 shows progressive changes in crack densities at the subject bridges. Ordinary concrete deck slabs often developed cracks in the early stages before they could be affected by vehicular load, amd the cracks steadily lengthened and widened with the passage of time. In contrast, expansive concrete deck slabs did not develop cracks until an age of about 18 months, and the number that did appear was far smaller than in the case of ordinary concrete. In addition,

Table 1 Outline of the investigated bridges

Type of bridge (bridge)	Name of bridge (Bridge)	Division of up and down lane	Kind of deck slab concrete (Concrete)	Length of bridge (m)	Angle of skew	Road width (m)	Main girder: Number (−)	Main girder: Interval (m)	Main girder: Height (m)	Deck slab: Thickness (cm)	Deck slab: Primary reinforcement (mm)	Deck slab: Distribution reinforcement (mm)	Deck slab: Kind of concrete (concrete)	Deck slab: Characteristic compressive strength of concrete (kgf/cm²)	Deck slab: Day placed concrete (date)
Simple composite girder bridge	Kuroishihama	down in ramp	Expansive	41.5	63	8.5	4	2.00	2.25	24.0	D19 125 ctc (cover 40)	D16 125 ctc (cover 40)	A_{1-3}	300	10/31/1980
	Suzumekura	up in ramp	Ordinary	38.95	70	8.5	4	2.576	2.20	23.0	〃	〃	A_{1-1}	300	10/17/1980
4-span continous non-composite plate girder	Tarami	down (part<1>) down (part<1>) up (part<1>)	Expansive Ordinary Ordenary	149.15 149.15 149.15	0 0 0	9.25 9.25 9.25	5 5 5	2.00 2.00 2.00	2.00 2.00 2.00	21.0 21.0 21.0	〃 〃 〃	〃 〃 〃	B_{0-3} B_{0-1} B_{0-1}	240 240 240	6/25/1982 6/25/1982 4/28/1982

Table 2 Specified mix of concrete and quality of placed concrete

Name of bridge (Bridge)	Division of up and down lane	Kind of deck slab concrete (Concrete)	Kind of concrete (Concrete)	Specified mix: Maximum size of coarse aggregate (mm)	Range of slump (cm)	Range of air content (%)	Water-cementitious material ratio W/(C+E) (%)	Sand-aggregate ratio s/a (%)	Unit content (kg/m³): Water W	Cement C	Expansive admixture E	Fine aggregate S	Coarse aggregate G	Air-entraining and water-reducing agent	Placed concrete: Slump (cm)	Air content (%)	Temperature (℃)	Compressive strength (28days) (kgf/cm²)
Kuroishihama	down in ramp	Expansive	A_{1-3}	25	8±2.5	4±1	41.2	40.0	160	345	35	699	1069	0.95	8.5	4.4	21	446
Suzumekura	up in ramp	Ordinary	A_{1-1}	25	8±2.5	4±1	41.2	40.0	160	380	0	699	1069	0.95	8.0	4.1	28	384
Tarami	down (part<1>) down (part<1>) up (part<1>)	Expansive Ordinary Ordenary	B_{0-3} B_{0-1} B_{0-1}	25 25 25	8±2.5 8±2.5 8±2.5	4±1 4±1 4±1	50.3 50.3 50.3	42.5 42.5 42.5	161 161 161	285 320 320	35 0 0	760 760 760	1051 1051 1051	0.80 0.80 0.80	8.3 8.8 8.6	4.5 4.0 3.9	30 32 25	331 335 337

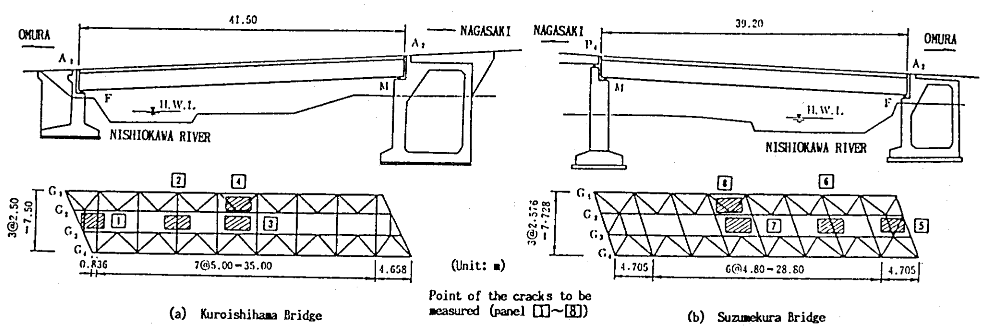

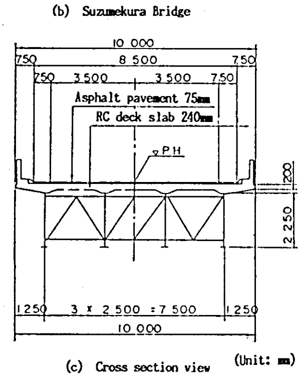

Fig. 1 Outline of simple steel composite girder (Kuroishihama Bridge and Suzumekura Bridge)

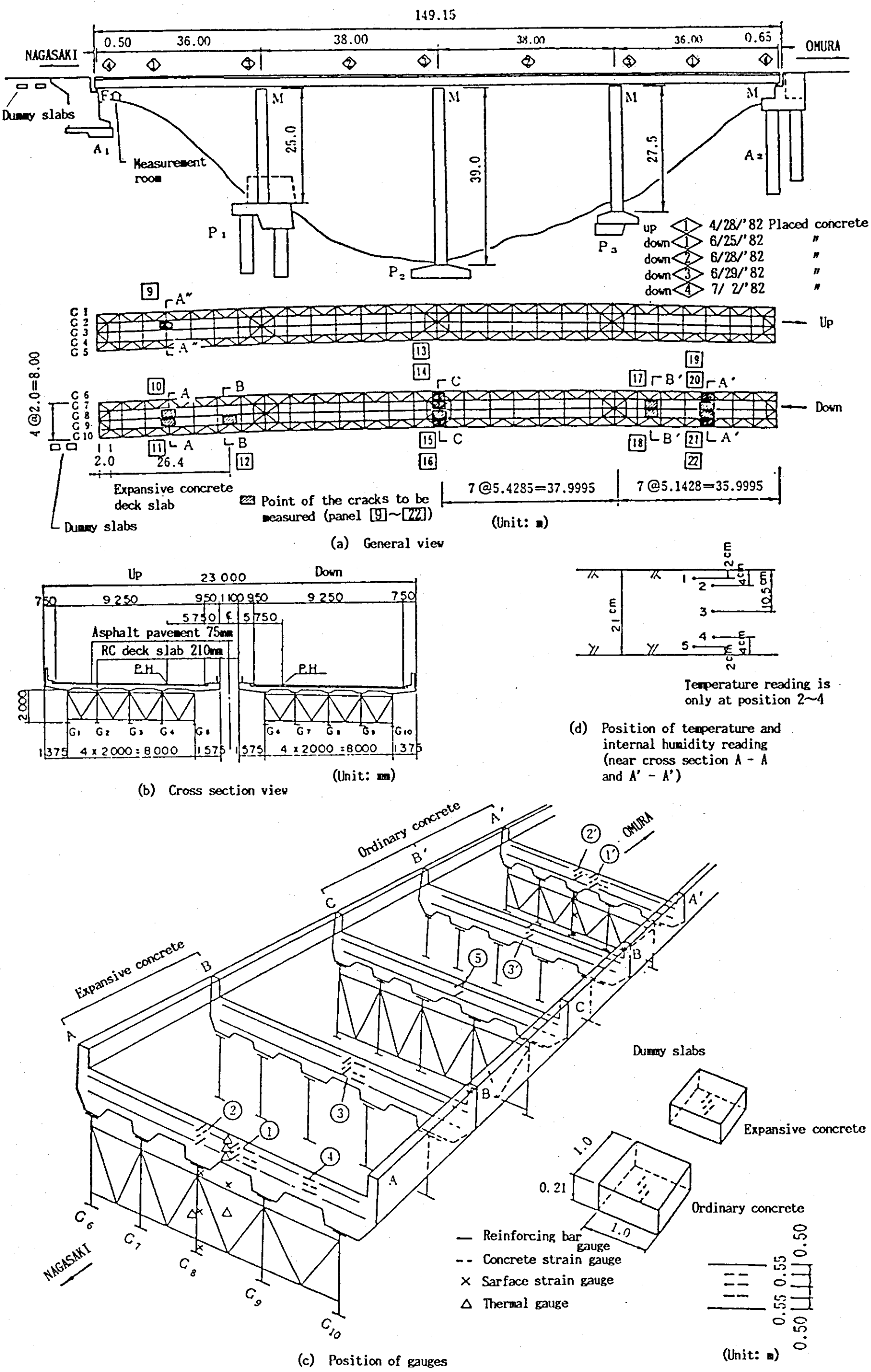

Fig.2 Outline of 4-span continuous steel non-composite plate girder (Tarami Bridge)

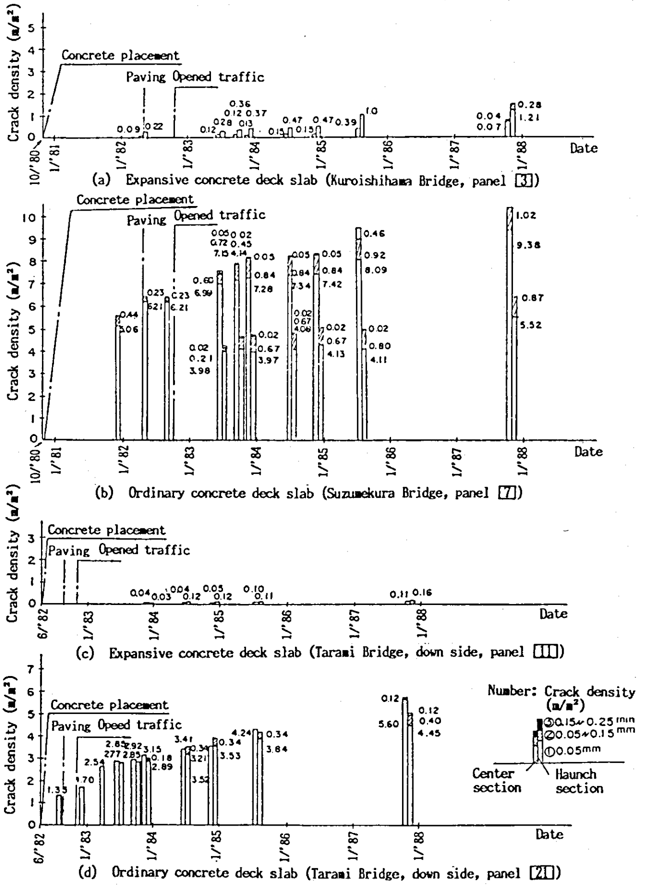

Fig. 3 Progressive changes in crack densities

nearly all were fine cracks of less than 0.05 mm, and the speed of growth was slower as well.

The deck slabs used in the simple steel composite girder and the 4-span continuous steel non-composite plate girder have reached an age of seven years and five and a half years, respectively. During this time, the trend in crack formation has remained more or less consistent and cracks have continued to progress at both bridges. As discussed below, this is thought to be due to the fact that the initial cracks that occurred as a result of drying shrinkage and temperature change continued to grow as the concrete aged and the effects of vehicular load were felt.

Figs. 4 and 5 and Table 3 summarize the cracking conditions observed at the subject bridges. These indicate the following tendencies:

1) Most of the cracks in expansive concrete deck slabs ran perpendicularly to the bridge axis and had not grown beyond their initial sizes.
2) The steel composite girder had roughly 1.5～2 times higher crack density than the steel non-composite girder. This is believed to be due to the use of studs for preventing slippage in the case of the former and slab anchor in the

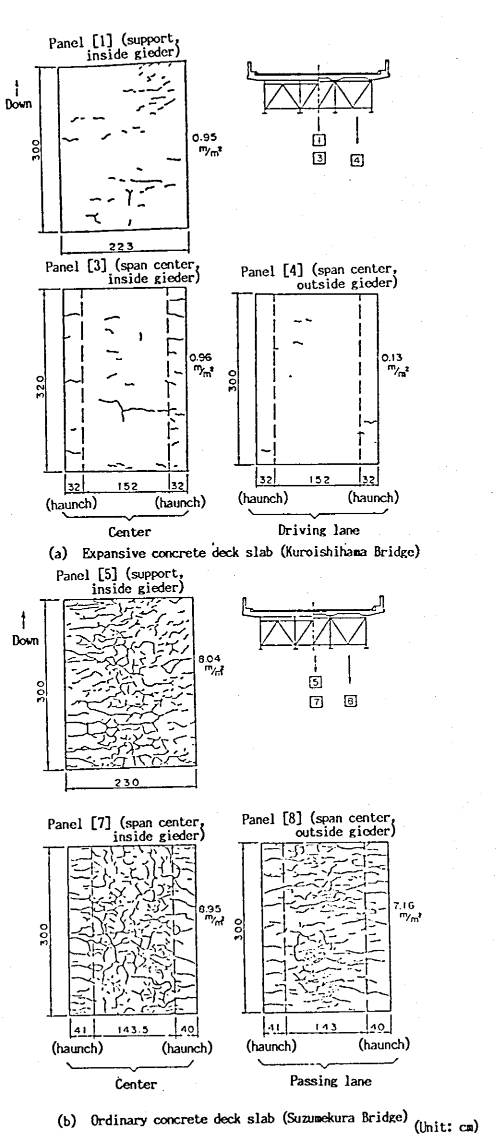

Fig.4 Cracking condition of siple composite girder bridge (Survey in November 1987, an age of 7 years)

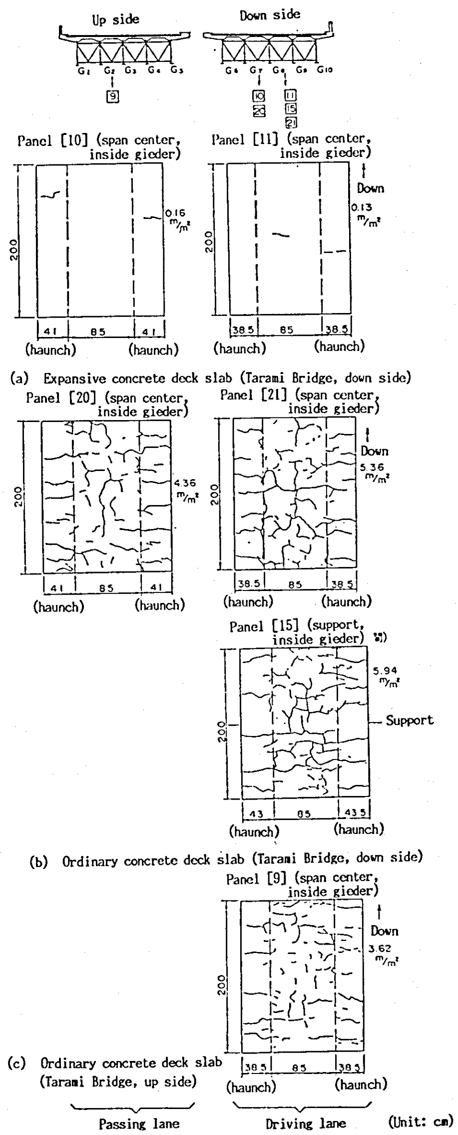

Fig.5 Cracking condition of 4-span continuous non-cmposite plate girder bridge (November 1987, an age of 5 years and 5 months)

case of the latter, resulting in a difference in the strength of restraint that girders fix deck slabs [9].

3) The cracking pattern differed in accordance with the conditions of restraint existing between steel girders and deck slabs. Crack formation in ordinary concrete deck slabs showed the following tendencies:

(a) Concerning the inner deck slabs (those located between two inside girders), most of the cracks in the haunch sections and in sections close to

Table 3 Crack densities (measureed in November 1987)

Division		Kind of deck slab concrete (concrete)	Surveyed point: Cross section	Traffic lane *	Panel	Relation on girders **	Crack density (m/m²) ***: Calculated by cracking length	Calculated by the grid density method: transverse direction	longitudinal direction	(Crack density in transverse direction) / (Crack density in longitudinal direction)
Composite	Kuroishihama Bridge	Expansive	Span center	Driving	4	Outside	0.13	0.10	0.00	—
				Center	3	Inside	0.96	0.82	0.29	2.77
			Near support	Center	1	Inside	0.95	0.87	0.38	2.31
	Suzumekura Bridge	Ordinary	Span center	Center	7	Inside	8.95	6.00	5.58	1.08
				Passing	8	Outside	7.16	6.07	2.55	2.38
			Near support	Center	5	Inside	8.04	5.83	4.38	1.33
Non-composite	Tarami Bridge	Expansive	A — A	Driveng	11	Inside	0.13	0.11	0.00	—
				Passing	10	Inside	0.16	0.13	0.06	2.31
		Ordinary	A' — A'	Driving	21	Inside	5.36	3.66	3.12	1.17
				Passing	20	Inside	4.36	3.50	2.17	1.61
			C — C	Driving	15	Inside	5.94	4.47	2.89	1.55
			A" — A"	Driving	9	Inside	3.62	3.00	1.50	2.00

* From the upper section, Driving, center (extends into driving lane and passing lane), and passing lane, in that order.
** Outside : Between a inside girder and outside one, Inside : Between the inside girders.
*** Which includes the haunch section.

the main girder occured in the primary reinforcement direction (perpendicular to bridge axis, hereafter the transverse direction), while most of the cracks in the center sections ran in the distribution reinforcement direction (parallel to bridge axis, hereafter the longitudinal direction).

(b) Since the outer deck slabs (those adjacent to an outside girder) are less restrained by steel girders in the transverse direction than the inner slabs, they showed hardly any cracks in the longitudinal direction, and their reaction, and their cracking densities were lower than those of inner slabs.

(c) In the continuous non-composite girder bridge, crack density was higher over the middle support than at span center. This is believed to be due to the fact that (i) the former area, being located above a pier, is more restrained by the steel girder in the transverse direction than the latter area, and (ii) owing to the effects of dead and live loads, tensile stress generated by the main girder in a deck slab located over the middle support acts in the longitudinal direction.

4) Crack densities were higher on the through lane than the passing lane. This is believed to be due to the repeated effects of vehicular load.

3.2 Expansive Properties and Chemical Prestress

Fig. 6 through 8 shows progressive changes in strain with respect to unrestrained dummy slabs and the subject bridge deck slabs (cross sections A-A and A'-A'). From the initial values obtained two hours after the placement of concrete, the chart plots each of the values obtained at the ages of one, two, three, seven, and 14 days and at one month, and the values obtained once a month thereafter up to an age of five years and six months. Values from one month onwards apply to 8:00 a.m. (once a day), when temperatrue variance inside a deck slab (depthwise) is small and thermal stress is weak.

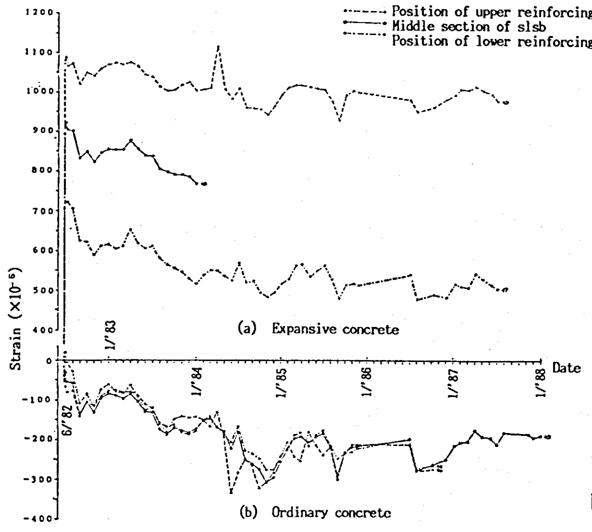

Fig. 6 Progressive change of dummy slabs

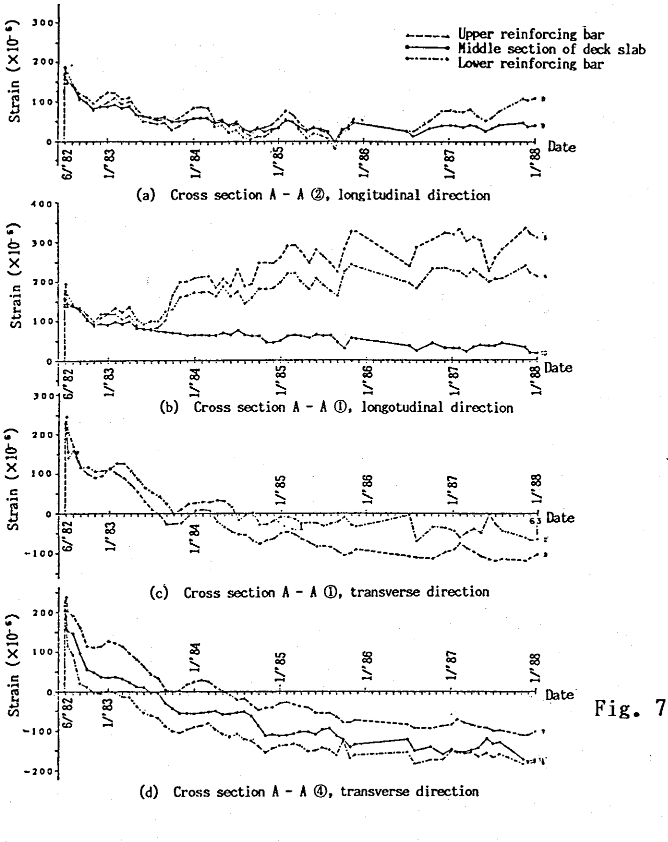

Fig. 7 Progressive change of of expansive concrete deck slabs (cross section A-A)

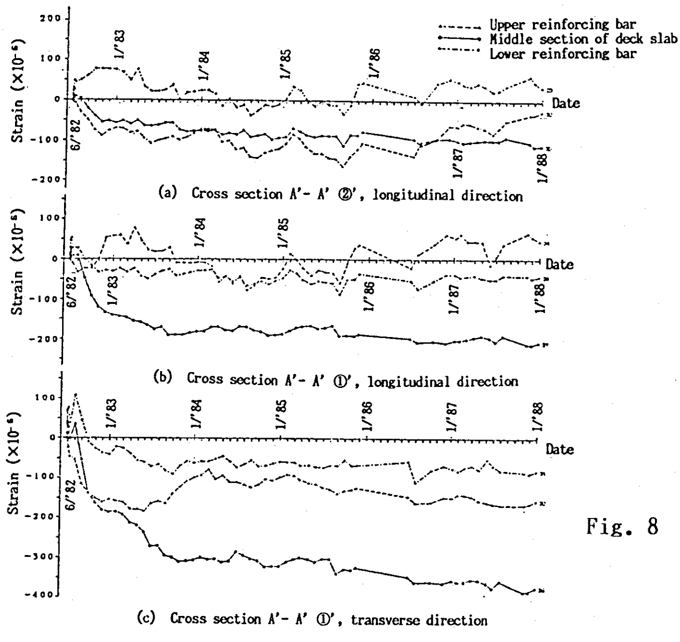

Fig. 8 Progressive change of ordinary concrete deck slabs (cross section A'-A')

Fig. 6 shows that maximum expansive strain in unrestrained dummy slabs was 1090×10^{-6} at the upper reinforcing bar position and 720×10^{-6} at the lower reinforcing bar position. In other words, the expansion rate was higher toward the upper surface, because of the weaker restraint provided by the frame. Unrestrained expansive strain in the subject bridge deck slabs is believed to roughly correspond to the upper bar value (1090×10^{-6}), which conforms to the specification cited in Recommended Practice [8] on the relationship between unit expansive admixture content and unrestrained expansion rate.

The amount of chemical prestress applied to the subject bridge deck slabs was estimated on the basis of the method developed by Tsuji [9], using the expansive strain values obtained from measurements (see Table 4). In cross section A-A, average expansive strain in the transverse direction, which is less restrained by the steel girder, was more or less the same for the inner slab ($G_8 \sim G_9$) and outer slab ($G_9 \sim G_{10}$). The latter, however, had a higher expansion rate toward its upper surface as in the case of dummy slabs. From these strain values, the amount of chemical prestress applied to the subject bridge deck slabs is estimated to be roughly 8 kgf/cm^2. Expansive strain in the longitudinal direction, which is greatly restrained by the steel girder, was nearly the same between girders ($G_8 \sim G_9$) and over a girder (G_8). Chemical prestress is estimated to be roughly 10 kgf/cm^2.

In contrast to cross section A-A, expansive strain in cross section B-B was greater in the longitudinal direction. This was because the survey point in cross section B-B was near the edge of a placing block (87 cm from the joint), and the adjacent concrete block was not placed until an age of four days.

3.3 Drying Shrinkadge and Internal Humidity

Humidity readings taken from the inside of deck slabs indicate that, both in the case of ordinary concrete and expansive concrete, the quantity of moisture loss

Table 4 Maximum expansive strain and chemical prestress of subject bridge deck slabs (an age of 3 days)

Division				Expansive strain ($\times 10^{-6}$)		Chemical prestress
Direction *1)	Cross section	Position in plane	Position in cross section *2)	Each value	Average value	(kgf/cm^2)
Transverse	A - A	① $G_8 \sim G_9$	Upper	226	228	7.9
			Middle	227		
			Lower	232		
		④ $G_9 \sim G_{10}$	Upper	230	207	7.2
			Middle	205		
			Lower	185		
	B - B	③ $G_8 \sim G_9$	Upper	214	182	6.3
			Middle	182		
			Lower	151		
Longitudinal	A - A	① $G_8 \sim G_9$	Upper	171	174	10.4
			Middle	171		
			Lower	179		
		② on G_8 girder	Upper	164	174	10.4
			Middle	171		
			Lower	187		
	B - B	③ $G_8 \sim G_9$	Upper	228	225	5.1
			Middle	221		
			Lower	225		

*1) Transverse : transversal direction (primary reinforcement direction))
Longitudinal: Longitudinal direction (distribution reinforcement direction)
*2) Upper : Upper reinforcing bar
Middle : Middle section of deck slab (concrete strain)
Lower : Lower reinforcing bar

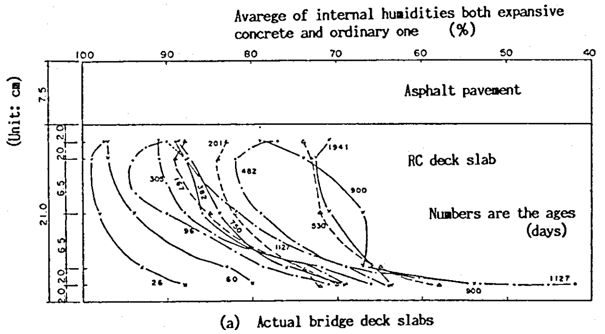

(a) Actual bridge deck slabs

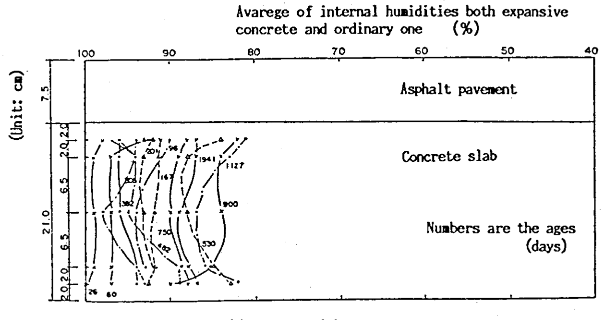

(b) Dummy slabs

Fig. 9 Change of internal humidity

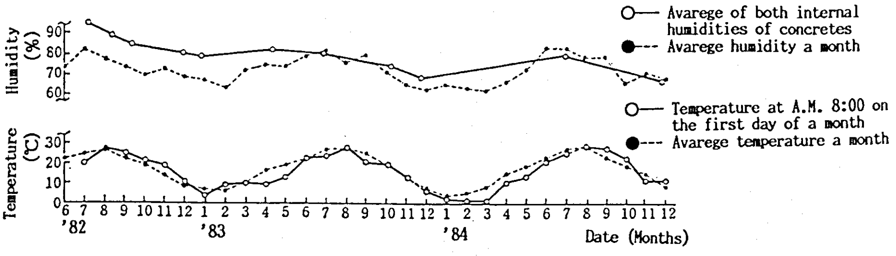

Fig. 10 Surroundings condition of subject bridge (data by Nagasaki Marine Meteorological Observatory) and average of internal humidities of concrete (both expansive and ordinary concrete deck slabs)

(drying) varies from top to bottom owing to the influence of such environmental factors as elevation (from ground), rainfall, sunlight, wind velocity, and surface paving, resulting in the disproportionate distribution of internal humidity [19],[20]. Fig. 9 shows the relationship between material age and average internal humidity (the average of readings taken near cross sections A-A and A'-A') for both expansive and ordinary concrete deck slabs. The internal humidity of the subject bridge deck slabs more or less corresponded to the monthly average of atmospheric humidity (see Fig. 10) from about two years onwards [14].

The maximum drying shrinkage strain of dummy slabs was only 240×10^{-6} even at an age of five years and six months (see Fig. 6). This figrue is lower than the unrestrained shrinkage strain of the subject bridge deck slabs ($300\sim500\times10^{-6}$) estimated from measurement results. This is believed to be due to the fact that the dummy slabs were located only 40cm from the ground, where the effects of rain and mist result in a humid environment (see Fig. 9).

The drying shrinkage strain of expansive concrete deck slabs in the subject bridges was approximately 360×10^{-6} in the transverse direction and 170×10^{-6} in the longitudinal direction (average values obtained from cross sections A-A and B-B; see Fig. 7). Thus, shrinkage strain was about 1.6 times greater than expansive strain in the transverse direction, which is less restrained by the main girder, and more or less the same in the longitudinal direction.

Ordinary concrete deck slabs in the subject bridges showed extensive cracking, and since strain gauges are affected by the existence of cracks, it is difficult to estimate the actual extent of drying shrinkage strain (strain without influence of cracks) in these slabs. Although concrete gauge①' at deck slab center indicated shrinkage strain of 410×10^{-6} in the transverse direction and 230×10^{-6} in the axial direction (see Fig. 8), the upper and lower bars shifted midway to the tension side due to the appearance of cracks. It is surmised that cracking served to somewhat reduce resistance against shrinkage in the concrete gauge vicinity and that shrinkage strain was actually slightly lower than the gauge figures. Therefore, We assume that the shrinkage strain of ordinary concrete was about the same as that of expansive concrete.

Drying shrinkage strain is considered to have virtually ended at an age of about three years while cracking is presumed to be still continuing due to the effects of vehicular load, in view of the facts that the strain values levelled off at an age of $2\sim3$ years (see Fig. 7 and 8); that the internal humidity of the subject bridge deck slabs more or less corresponded to atmospheric from about two years onwards, as mentioned above; and that the relationship between internal

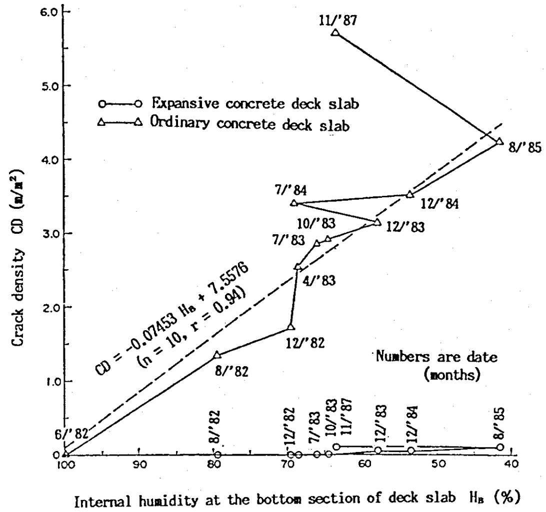

Fig. 11 Relationship between internal humidity (2 cm from bottom surface of deck slab, Fig. 2(d)) and cracking density

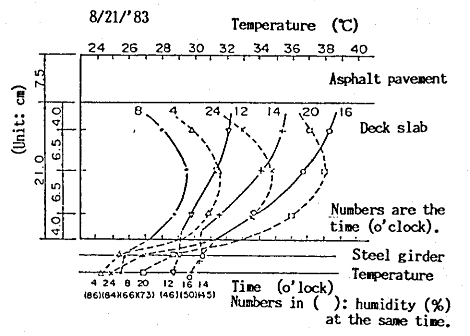

Fig. 12 Example of change of internal temperature in a day (in summer)

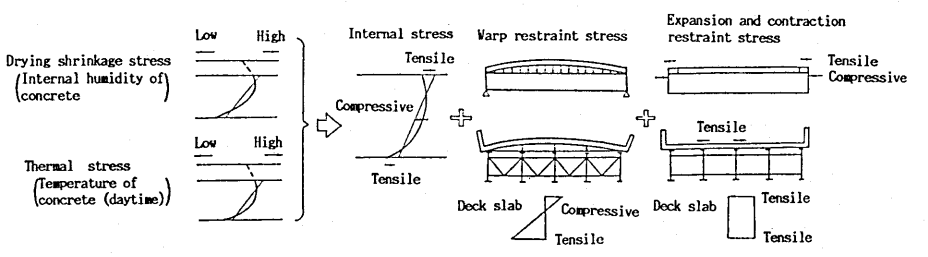

Fig. 13 Illustration of Drying Shrinkage Stress and Thermal Stress

humidity and cracking density was more or less a straight line up to about three years (see Fig. 11).

3.4 Internal Temperature of Deck Slabs

Temperature readings obtained from the insides of deck slabs indicate that the distribution of internal temperature, like that of internal humidity, was not evenly balanced owing to the influence of such environmental factors as sunlight, atmospheric temperature and surface paving [12], [14]. Fig. 12 gives an example of this: internal temperature showed the greatest fluctuation in the summer, when atmospheric temperature rises sharply, while strain in the lower reinforcing bar shifted to the tension side in the daytime (see Fig. 18 and Fig. 19 below).

4. INITIAL CRACKING MECHANISM OF RC DECK SLABS OF STEEL BRIDGES

4.1 Stresses in RC Deck Slabs of Steel Bridges

(1) General Concept on Causes of Initial Cracking

Taking into account the fact that RC deck slabs showed cracks before vehicular load affected the slags, as indicated by the survey results discussed above, the primary causes for initial cracking are thought to include the drying shrinkage of concrete and temperature change caused by exposure to sunlight. Fig. 13 illustrates the effects of drying shrinkage stress and thermal stress. Both generate tensile stress at the bottom surface of a deck slab during the day owing to the disproportionate perpendicular distributions of internal humidity and internal temperature [21].

To explain further, in drying shrinkage, the lower side of a deck slab dries much faster than the upper side, as shown in Fig. 9, so that the deck slab tries to deform in such a way that it projects convexly upwards. But this deformation is restrained by the steel girder, resulting in tensile stress in at the bottom surface. As for temperature change, the farther away a given point in a deck slab is from its top surface, which receives sunlight, the longer it takes for its temperature to change. In the daytime, therefore, temperature change progresses from top to bottom (upper reinforcing bar, middle section, lower bar, and steel girder in that order), causing the deck slab to try to project upwards (see Fig. 12). But this deformation is again restrained by the steel girder, resulting in tensile stress at the bottom surface of the deck slab. At the same time, internal stress is generated by the curvilinear distribution of internal temperature.

(2) Analyzing Method on Restraint of Girder

A concrete deck slab connected to a steel girder by a slab anchor (a stud is used with a composite girder) undergoes thermal stress due to a restraining mass when it is affected by the king of temperature variance shown in Fig. 14. Since the compensation line method has been used in the past to analyze thermal stress in mass concrete [22], [23], the method was used here also.

The Young's modulus and coefficient of heat expansion for a concrete deck slab are considered to become constant when the concrete hardens. Accordingly, the following relationships can be obtained from Fig. 14:

$$\bar{\varepsilon} = \alpha / H \cdot \int T(y)\,dy \tag{1}$$

$$\phi = \alpha \cdot \frac{\int T(y)\,y\,dy}{\int y^2\,dy} \tag{2}$$

Where H : Thickness of concrete structure (cm)
α : Coefficient of heat expansion for concrete (1/℃)
T(y) : Distribution of temperature difference (℃)

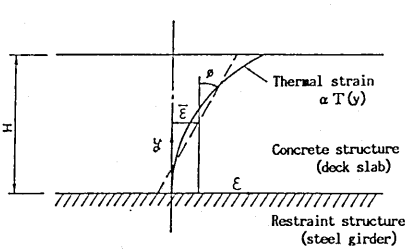

Fig. 14 Idea of compensation Line

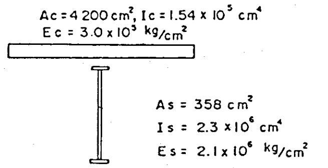

Fig. 15 Values of representative cross section of Tarami Bridge

$\bar{\varepsilon}$: Strain related to axial force (−)
ϕ : Gradient of strain related to flexual diformation (cm^{-1})

When the free deformation of a concrete deck slab is inhibited by a restraining mass (steel girder), the latter is considered to be an elastic body and the force of restraint is expressed as axial force N and bending moment M defined by the following equations:

$$N = R_N \cdot N_0 = R_N \cdot A_C \cdot E_C \cdot \bar{\varepsilon} \quad (3)$$
$$M = R_M \cdot M_0 = R_M \cdot I_C \cdot E_C \cdot \phi \quad (4)$$

Where N_0 : Axial force assuming a completely rigid restraining mass (absolute axial restraint)
M_0 : Flexual moment assuming a completely rigid restraining mass (hereafter referred to as absolute flexual restraint)
R_N : Coefficient expressing the strength of restraint on deformation in the longitudinal direction (hereafter referred to as factor of axial restraint)
R_M : Coefficient expressing the strength of restraint on flexual deformation (hereafter referred to as factor of flexual restraint)
A_C : Cross sectional area of concrete deck slab
E_C : Young's modulus of concrete deck slab
I_C : Moment of inertia of concrete deck slab

Dividing into the longitudinal direction and transverse one, R_N and R_M were calculated as follows based on the relationship between deck slab rigidity and steel girder rigidity:

a) Longitudinal direction

The following calculations were made on a representative cross section of Tarami Bridge (non-composite girder), shown in Fig. 15. First, R_N was obtained in a simple manner from the following equation based on the concept of thermal stress in a composite cross section.

$$R_N = 1 - \frac{E_C A_C}{E_C A_C + E_S A_S} = 0.37 \fallingdotseq 0.4 \quad (5)$$

Where Es : Young modulus of steel girder
As : Cross sectional area of steel girder

In the same way, R_M was obtained in a simple manner from the following equation based on the relationship between the flexual rigidity of a deck slab alone and the flexual rigidity of a composite cross section (deck slab plus steel girder).

$$R_M = 1 - \frac{E_C I_C}{E_S I_V} = 0.996 \fallingdotseq 1.0 \quad (6)$$

Where I_V : Composite moment of inertia {(deck slab converted into steel) + (steel girder)}

b) Transverse direction

The same procedure was followed for representative cross section of Tarami Bridge in the main bar direction, shown in Fig. 2(b), to obtain the factor of axial and flexural restraint.
Steel member found in the main bar direction consist entirely of sway bracing placed 5~6 meters apart, and only the top chord members are considered to resist the expansion and shrinkage of deck slabs. Therefore, Ac = (deck slab thickness) × (sway bracing interval)= 10,500 cm^2 and As= (cross sectional area of top

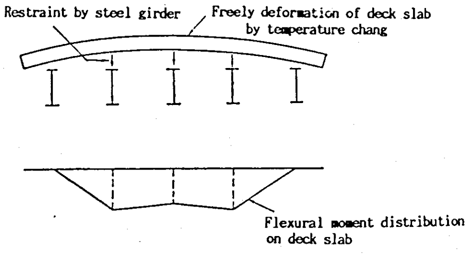

Fig.16 Flexural noment of deck slab caused by restraint of steel girder

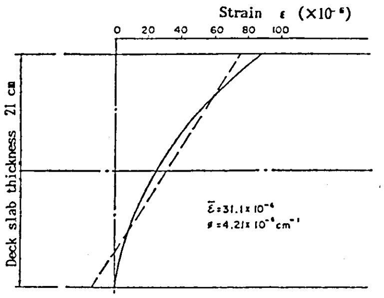

Fig.17 Compensation Line on temperature change

chord member of sway bracing)= 37.87 cm^2. When these values are substituted in equation (5) the result is a virtual zero, indicating that restraint is negligible:

$$R_N = 0.025 \fallingdotseq 0$$

As for bending in the transverse direction, deck slabs are restrained at each main girder position, resulting in the flexural moment distribution shown in Fig. 16. The flexual moment is zero at the projecting edges and above outside girders, and more or less uniform between girders. Main girder restraint is extremely strong at the support and weaker along the span owing to the fact that the girder sags slightly at the span. However, since the flexual rigidity of main girders was found to be sufficiently higher than that of deck slabs, as mentioned in a) above, factor of flexural restraint in the transverse direction, including the span area, is considered to be:

$$R_M \fallingdotseq 1.0$$

In the case of the composite girder bridge subject to this study, the values obtained were comparable to the above values. However, since studs rather than bracing are used to prevent slippage, restraint is assumed to be greater than in the case of the non-composite girder bridge [9].

4.2 Calculation of Thermal Stress

The compensation line shown in Fig. 17 was obtained on the basis of temperature difference between 8:00 and 16:00 as indicated by Fig. 12, which shows how temperature distribution in a deck slab changed during the day at the Tarami Bridge, and the actually-measured coefficient of heat expansion for concrete (9.5×10^{-6}/℃). From this the following values were obtained:

$$\varepsilon = 31.1\times10^{-6}$$
$$\phi = 4.21\times10^{-6}\ \mathrm{cm}^{-1}$$

It follows, then, that absolute axial and bending restraints per unit of width are:

$$N_0 = 1.96\times10^4\ \mathrm{kgf/m}$$
$$M_0 = 9.75\times10^4\ \mathrm{kgf\cdot cm/m}$$

a) Deck slab stress in longitudinal direction

Member force and flexual moment in the longitudinal direction were calculated from the above-mentioned restraint factors R_N and R_M and absolute restraints N_0 and M_0 as follows:

$$N = R_N\times N_0 = 0.4\times1.96\times10^4 = 7840\ \mathrm{kgf/m}$$
$$M = R_M\times M_0 = 1.0\times9.75\times10^4 = 97500\ \mathrm{kgf\cdot cm/m}$$

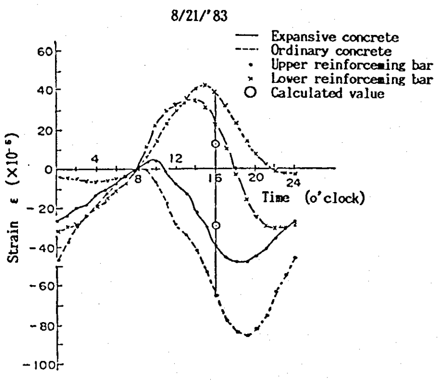

Fig.18 Comparison between surveyed values and calculated values (distribution reinforcement)

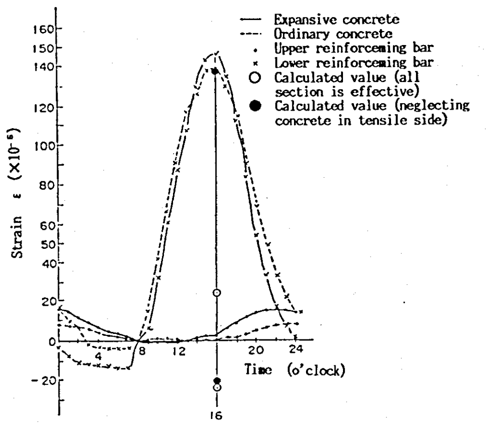

Fig.19 Comparison between surveyed values and calculated values (primary reinforcement)

Assuming that the entire cross section of deck slab concrete is effective, stresses at the top and bottom surfaces of a deck slab were calculated based on axial force N and flexual moment M and added to internal stress, resulting in -20.9 kgf/cm^2 (compression) at the top surface and 5.8 kgf/cm^2 (tension) at the bottom surface. The strains of the upper and lower reinforcing bars, then, are -29×10^{-6} (compression) and 12×10^{-6} (tension) respectively, as shown in Fig. 18. These values are slightly smaller than the measured values.

b) Unit stress in transverse direction

Axial force and flexual moment in the main bar direction were calculated as follo ws:

$$N = R_N \times N_0 \fallingdotseq 0$$
$$M = R_M \times M_0 = 1.0\times9.75\times10^4 = 97500 \text{ kgf·cm/m}$$

Again, assuming that the entire cross section of deck slab concrete is effective, stress at the top and bottom surfaces of a deck slab was calculated and added to internal stress, resulting in -16 kgf/cm^2 (compression) at the top surface and 8 kgf/cm^2 (tension) at the bottom surface. The strains of the upper and lower reinforcing bars in this case came to -24×10^{-6} (compression) and 23×10^{-6} (tension), respectively. On the other hand, if the tension side of the deck slab is neglected, stress at the top surface comes to -20 kgf/cm^2 (compression) and stress at the tension side of the reinforcing bar comes to 285 kgf/cm^2. In this case, strains of the upper and lower reinforcing bars are -21×10^{-6} (compression) and 136×10^{-6} (tension) respectively.

Fig. 19 compares the calculated values mentioned above with the measured values. It can be seen that the measured values are close to the values obtained when the tension side of concrete was neglected. According to a measurement conducted in December 1983, a tiny crack was observed near the strain gauge placed in expansive concrete. As in the case of ordinary concrete, it is believed that this condition caused the measured value to approximate the value calculated without the tension side.

Based on the foregoing, it is believed that temperature change during the day generated tensile stress of around 6 kgf/cm^2 in the longitudinal direction and 8

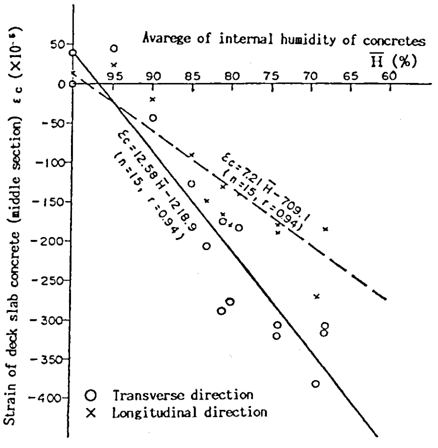

Fig. 20 Relationship between average internal humidity and strain of deck slabs

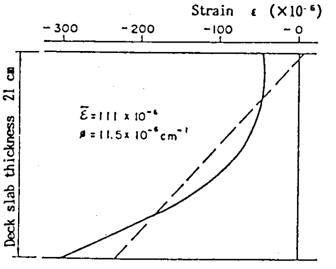

Fig. 21 Compensation Line on drying shrinkage

Table 5 Calculated values of deck slab stresses caused by drying shrinkage

Position in deck slab		Deck slab stress (kgf/cm²) *
Direction	Position in cross section of deck slab	
Transverse	Top surface Bottom surface	-14 40
Longitudinal	Top surface Bottom surface	-4.5 49

* $\phi=1.2$

Table 6 Example on calculated values of stresses generated at bottom surface of deck slabs (in the case that concrete is plased in summer and it continue fine weather)

(unit : kgf/cm²)

Items		Expansive concrete deck slab		Ordinary concrete deck slab	
		Transverse	Longitudinal	Transverse	Longitudinal
Deck slab stress	Dead loads Thermal stress (daytime) Drying shrinkage (age 60days) Chemical prestress	3 8 40 -8	— 6 49 -10	3 8 40 —	— 6 49 —
	Subtotal	43	45	51	55
	Wheel load	27	21	27	21
	Total	70	66	78	76
Strength	Flexural strength	47 (58)		48 (54)	
	Tensile strength	32 (37)		31 (35)	
*)	Compressive strength	363 (422)		367 (399)	

*) Test value by specimens cured under the field conditions. age 28 days, ( ) : age 91 days.

kgf/cm² in the transverse direction in the summer.

4.3 Calculation of Drying Shrinkage Stress

The average internal humidity of deck slabs was obtained from the data given in Fig. 9 and charted in relation to concrete strain, as shown in Fig. 20. The shrinkage factors (the gradients of the charted lines) obtained from this chart were 12.58×10^{-6} in the transverse direction and 7.21×10^{-6} in the longitudinal direction. The value is smaller in the direction in which the steel girder provides greater restraing (longitudinal direction). The value for the transverse direction is comparable to the lengthwise deformation rate per unit of humidity, 14×10^{-6}, obtained from plain concrete [19].

Taking the humidity distribution at an age of 60 days given in Fig. 9 as an example, the shrinkage coefficient in the transverse direction of 12.58×10^{-6} which is close to the value for free deformation, was used to calculate the compensation line shown in Fig. 21. From this, the following values were obtained:

$$\varepsilon = 111\times10^{-6}$$
$$\phi = 11.5\times10^{-6}\ \mathrm{cm}^{-1}$$

Assuming that at this stage there are no cracks in the deck slab and that the concrete cross section alone offers resistance, deck slab stress due to external restraint was calculated based on the above-mentioned restraint coefficients. Internal stress was then added to the value thus calculated to arrive at deck slab stress generated by drying shrinkage (see Table 5). Creep was taken into account in the calculation by assuming a creep factor of ϕ = 1.2 based on the results of a creep test conducted on expansive concrete speciments at an age of 60 days, and using the creep coefficient to reduce the Young's modulus for concrete.

In this way, it was quantitatively confirmed that drying shrinkage has a much greater influence on deck slab stress than temperature change, both in terms of strength of change and disproportionate distribution within a deck slab.

4.4 Generating Stesses in a deck slab

The various factors that generate stress in a deck slab are listed in Table 6. These consist of dead load and vehicular load (live loads) calculated in accordance with Specification of Highway Bridges [24], the chemical prestress mentioned earlier, and drying shrinkage stress and thermal stress calculated as per the above.

From the foregoing we were able to confirm that, after moist curing and along with the removal of formwork and shoring, temperature change and drying shrinkage affect RC deck slabs, creating a substantial tensile stress at their bottom surfaces prior to the effects of vehicular load and leading to the development of initial cracks. In the same way, if a deck slab is exposed to strong sunlight or wind without receiving adequate curing treatment immediately after placement, the top surface of the deck slab easily undergoes tensile stress, resulting in the formation of cracks. In fact, there have been a few cases where penetrating cracks had formed in the concrete even before formwork removal, owing to an initial curing process that did not take into account the severe weather conditions that existed at the time of placement.

The values shown in Table 6 are the results of sample calculations in which a combination of fairly severe conditions of stress was assumed, as mentioned above. The actual conditions for crack formation differ according to the bridge environment, design method, the quality of concrete (especially the unit water content), weather conditions on the day of placement, curing method, timing and method of asphalt paving, and other factors.

5. CONSIDERATION OF DESIGN VALUES FOR EXPANSIVE CONCRETE DECK SLABS

5.1 Consideration on Flexural Cracks

In determining the design values for RC deck slabs, the width of flexural crack

(w) at the serviceability limit state can be reduced by the use of expansive concrete. Standard Specification for Desin and Construction of Concrete Structures published by JSCE prescribe the following formula [25], which is based on past experiments, for calculating the width of flexural crack:

$$w = k_1 \{4c + 0.7 (c_s - \phi)\} \cdot \left[\frac{\sigma_{se}}{E_s} \left(\text{or } \frac{\sigma_{pe}}{E_p} \right) + \varepsilon'_{cs} \right] \qquad (7)$$

Where k_1 : Constant to take into account the influence of bond characteristics of steel, which may be set equal to 1.0 for deformed bars, 1.3 for plain bars and prestressing steel

c : Concrete cover (cm)

c_s : Center-to-center distance of steel (cm)

ϕ : Diameter of steel bar (cm)

σ_{se} : Increase of stress in reinforcing bar (kgf/cm^2)

E_s : Modulus of elasticity of reinforcing bar (kgf/cm^2)

σ_{pe} : Increase of stress in prestressing steel (kgf/cm^2)

E_p : Modulus of elasticity of prestressing steel (kgf/cm^2)

ε'_{cs} : compressive strain for evaluation of increment of crack width due to drying shrinkage and creep in concrete

In the above equation, ε'_{cs} is generally established as about 150×10^{-6} based on the investigation results of steel railway bridge [25], [26].

For experimental purposes, Kakuta's and Ozaka's equations are available [27], [28]. Using the former and also taking into account the measured values on strain, calculation trials of the ε'_{cs} values for expansive and ordinary concrete were made.

Since σ_{cm} (decline in reinforcing bar stress between cracks due to bonding of reinforcing bar and concrete, with said decline converted into average tensile stress of effective concrete cross section) = 0 against long-term continuous load in Kakuta's formula, and since expansive strain ε'_{scp} generated by chemical prestress acts against the cracking of expansive concrete deck slabs, the maximum crack width was calculated as follows:

$$w_{max} = \left(\frac{\sigma_s}{E_s} + \varepsilon_\phi \right) \cdot l_{max} \qquad \text{(ordinary concrete)} \qquad (8)$$

$$w_{max} = \left(\frac{\sigma_s}{E_s} + \varepsilon_\phi - \varepsilon'_{scp} \right) \cdot l_{max} \qquad \text{(expansive concrete)} \qquad (9)$$

The ε'_{cs} value given in the Standerd Specification [25] corresponds to ε_ϕ and ($\varepsilon_\phi - \varepsilon'_{scp}$) in the above formula. A flow chart showing the calculation procedure for ε'_{cs} is given in Fig. 22.

5.2 Trial calculation of ε_ϕ

For expansive concrete deck slabs, ε_ϕ was established as the elastic strain differential between reinforcing bar and deck slab caused by drying shrinkage and creep in the concrete mass (see Equation (10) below), under the assumption that there are no cracks in the deck slab.

$$\varepsilon_\phi = \varepsilon_s + \frac{\sigma_{c\phi}}{E_c} \qquad (10)$$

where ε_s : Deck slab strain caused by drying shrinkage

$\sigma_{c\phi}/E_c$: Strain corresponding to stress occurring in concrete due to drying shrinkage

Calculations of ε_s and $\sigma_{c\phi}/E_c$ were based on unrestrained drying shrinkage strain ε_0, as described below.

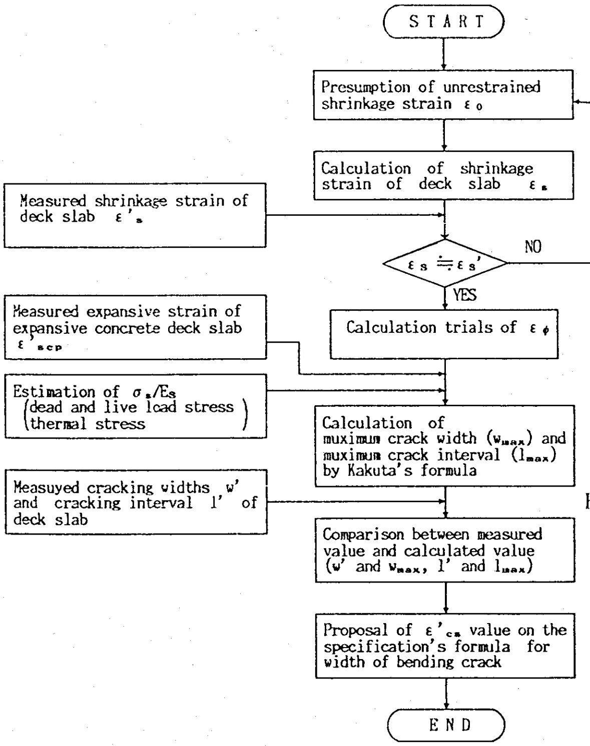

Fig. 22 Flow chart showing the calculation procedure for ε'_{cs}

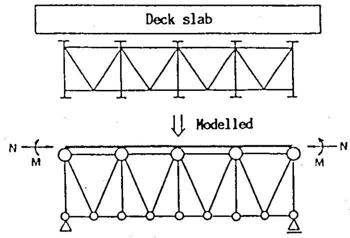

Fig. 23 Model for calculation of ε_{ϕ} in the transverse direction

For ordinary concrete deck slabs, ε_{ϕ} was established as unrestrained shrinkage strain ε_0, based on the consideration that these slabs developed crakcs at an early age.

Since the actually measured strain values for dummy slabs are unreliable, unrestrained shrinkage strain ε_0 was determined by tentatively establishing an ε_0 value and using that value to calculate ε_s in Equation (11). The ε_0 value which resulted in an ε_s value that closely matched drying shrinkage strain ε'_s obtained from the subject bridges was then used in subsequent calculations.

(1) Calculation procedure of ε_{ϕ} for expansive concrete deck slabs

a) ε_{ϕ} in the transverse direction

When calculating ε_{ϕ} in the transverse direction, the fact that the deck slab concrete, reinforcing bar, and sway bracing restrain the deformation of each other was taken into account. Calculations were made in two stages as described below (see Fig. 23).

① First, taking only the deck slab, shrinkage strain ε_{s1} generated in a deck slab due to restraint from its reinforcing bars when the deck slab concrete shrinks up to unrestrained shrinkage strain ε_0 was calculated.
② Restraint provided by sway bracing was then considered. A model framework of a deck slab and sway bracing was prepared, and shrinkage strain ε_{s2} gener-

ated in a lower reinforcing bar when its deck slab shrinks only up to ε_{s1} was calculated.

Shrinkage strain ε_{s2} obtained from ② above corresponds to final deck slab shrinkage strain ε_s :

$$\varepsilon_s = \varepsilon_{s2} \tag{11}$$

It follows, then, that tensile stress $\sigma_{c\phi}$ by concrete at the lower reinforcing bar position is:

$$\sigma_{c\phi} = (\varepsilon_0 - \varepsilon_s) \cdot E_c \cdot 2 / (2 + \phi) \tag{12}$$

Therefore, ε_ϕ in the transverse direction is:

$$\varepsilon_\phi = \varepsilon_s + \sigma_{c\phi} / E_c \tag{13}$$

b) ε_ϕ in the longitudinal direction

To calculate ε_ϕ in the longitudinal direction, the fact that the deck slab concrete, reinforcing bar, and girder restrain the deformation of each other and that the deformation of the overall bridge is restrained at the support were taken into consideration. Calculations were made in three stages as described below. ① First, taking only the deck slab, shrinkage strain ε_{s1} generated in a deck slab due to restraint from its reinforcing bars when the deck slab concrete shrinks up to unrestrained shrinkage strain ε_o was calculated.
② Restraint provided by a girder was then considered. Assuming a composite girder, shrinkage strain ε_{s2} generated in a lower reinforcing bar when its deck slab shrinks only up to ε_{s1} was calculated.
③ Restraint Provided by a support was then considered. In other words, the effect of restraining at a support deformation caused by bending moment M_{v2} in a rigid cross section, as obtained from ② above, was considered. Statically indeterminate flexural moment ΔM, which occurs in a given cross section when M_{v2} acts on a continuous girder, was calculated, after which shrinkage strain ε_{s3} generated in a lower reinforcing bar by ΔM was obtained.

Shrinkage strains ε_{s2} and ε_{s3} obtained from ② and ③ above correspond to final lower bar shrinkage strain ε_s:

$$\varepsilon_s = \varepsilon_{s2} + \varepsilon_{s3} \tag{14}$$

Tensile stress (σ_c) of concrete at the lower reinforcing bar position can then be obtained from Equation (12), and ε_ϕ in the longitudinal direction from Equation (13).

(2) Calculation results of ε_ϕ

The calculated values for drying shrinkage strain (ε_s) are compared with the measured values for drying shrinkage strain (ε's) in Table 7. Unrestrained shrinkage strain ε_0 is estimated to be about $300 \sim 500 \times 10^{-6}$. Accordingly, the middle ε_o value, 400×10^{-6}, was used to calculate ε_ϕ, and the results (ε_ϕ) are shown in Table 8.

In these calculations, the creep factor was established as 2.0, based on the results of creep tests conducted on expansive concrete specimens at an age of 1941 days.

5.3 Consideration of ε'_{cs} in Formula of the Width of Flexural Crack

The values for ε_ϕ (ordinary concrete) and $\varepsilon_\phi - \varepsilon'_{scp}$ (expansive concrete) given in Table 8 correspond to ε'_{cs} in Standard Specification [25]. Accordingly, the values for ε'_{cs} based on the above calculations are as shown in Table 9.

Calculations of maximum crack width w_{max} were made on the basis of Kakuta's and Ozaka's formulas, using the ε_ϕ values calculated as per 5.2; the design values for reinforcing bar stress generated by dead loads; the measured values for

Table 7 Comparison between calculated drying shrinkage strain (ε_s) and measured drying shrinkage strain (ε'_s)

Direction	Position in cross section	Calculated shrinkage strain ε_s (×10⁻⁶) Calculation equation	Unrestrained shrinkage strain ε_0 (×10⁻⁶) 300	350	400	450	500	Measured shrinkage strain ε'_s (×10⁻⁶)
Transverse	Upper	$0.8319\varepsilon_0$	250	291	333	374	416	340~370
	Middle	$0.8049\varepsilon_0$	241	282	322	362	402	360
	Lower	$0.7766\varepsilon_0$	233	272	311	349	388	360
Longitudinal	Middle	$0.5342\varepsilon_0$	160	187	214	240	267	160~180

Note) $\phi=2.0$

Table 8 Calculation results of ε_ϕ

(unit : $\times10^{-6}$)

Direction	Expansive concrete	Ordinary concrete
Transverse	355	400
Longitudinal	305	400

Note) $\phi=2.0$

Table 9 Calculation results of ε'_{cs}

(unit : $\times10^{-6}$)

Direction	Expansive concrete	Ordinary concrete
Transverse	135	400 (355~400)
Longitudinal	125	400 (305~400)

Table 10 Calculated values of maximum crack widths

Case	Calculation equation	ε'_{cs} (×10⁻⁶) *4) Expansive concrete	Ordinary concrete	Calculated crack widths (mm) *4) Expansive concrete	Ordinary concrete
[1]	Specification' formula equation (7) *1)	0 0	150 150	0.05 0.04	0.09 0.07
[2]	Specification' formula equatuon (7) *2)	125 135	400 400	0.12 0.09	0.15 0.15
[3]	Kakuta's formula equation (8)&(9)	125 135	400 400	0.12 0.07	0.19 0.10
[4]	Ozaka's formula *3)	125 135	400 400	0.09 0.06	0.17 0.10

*1) $k_1=1.0$, $k_2=0.5$, *2) $k_1=1.0$, $k_2=1.0$,
*3) $k=0.6$, $r=1.0$, $\zeta=0.6$,
*4) Upper section : correspond to the crack in transverse direction
Lower section : correspond to the crack in longitudinal direction

Table 11 Measured values of maximum crack widths

(unit : mm)

Direction	Expansive concrete	Ordinary concrete
Transverse	less than 0.05	0.15~0.25
Longitudinal	less than 0.05	0.05~0.15

reinforcing bar stress σ_s generated by temperature change; and the measured values for expansive strain ε'_{scp} at the subject bridges. Table 10 compares the w_{max} values thus calculated and the corresponding values obtained from the equation given in Standerd Specification [25].

Maximum crack widths in Cases [2]~[4], which are based on ε_ϕ (ε'_{cs}, ε'_{scp}) calculated from measured strain, are comparable to the maximum crack widths measured at the subject bridges (see Table 11). In Case [1], on the other hand, in which ε'cs is established as 150×10^{-6} (0 for expansive concrete), the maximum crack width of ordinary concrete is somewhat smaller than the measured figure.

While Standerd Specification [25] cites an ε'cs value of 150×10^{-6} for general application, in the case of Tarami Bridge about 130×10^{-6} for expansive concrete and 400×10^{-6} for ordinary concrete are believed to be more appropriate in view of the foregoing. In this study, the ε_ϕ value for ordinary concrete was assumed to be equivalent to unrestrained shrinkage strain $\varepsilon_0 = 400\times10^{-6}$, owing to the fact that cracking was observed in the initial stage. However, in a case where cracking develops after drying shrinkage has progressed to a certain extent, the ε_ϕ value should correspond to the elastic strain differential between a deck slab and its reinforcing bars. In view of this factor, ε'_{cs} for ordinary concrete is surmised to range between 300×10^{-6} and 400×10^{-6}, as shown within brackets in Table 9.

From the foregoing, it is believed that the use of expansive concrete (chemical prestressed concrete) allows the reduction of the ε'_{cs} value for RC deck slabs in steel highway bridges by $200\sim300\times10^{-6}$. In other words, the study proved that tensile strain in a reinforcing bar brought on by bending moment continues to decline even after the appearance of bending cracks, and that strength of this strain is nearly the same as the initial strain generated by the effects of expansion in the tensile-side reinforcing bar [8]. In addition, when using 150×10^{-6} as the design value for ordinary concrete, as is the practice at present, $\varepsilon'_{cs} = 0$ is believed to be appropriate for considering bending cracks in expansive concrete (chemical prestressed concrete).

6. CONCLUSION

The following conclusions can be obtained by this study:

(1) The use of expansive concrete (chemical prestressed concrete) in the RC deck slabs of steel bridges results in a significant reduction in crack formation compared to the use of ordinary concrete, and is an effective method for improving the durability of deck slabs.

(2) The RC deck slabs of steel bridges show disproportionate distributions of internal temperature and humidity from the initial stages owing to temperature change and drying shrinkage.

(3) Because steel girders restrain the deformation of deck slabs originating in (2) above, the latter undergoes thermal stress and drying shrinkage stress, developing cracks even without the effects of vehicular load. This effect is particularly pronounced in the early stages, when the concrete has not yet developed enough tensile strength.

(4) Due to (3) above, the bottom surface of a deck slab undergoes tensile stress in the daytime (especially in the dry season). For this reason, stress is at its greatest when vehicular load acts on a deck slab during the day. In addition, the disproportionate distribution of internal humidity becomes more pronounced with the passage of time, increasing tensile stress at the deck slab bottom.

(5) The strength of restraint provided by a steel girder in the transverse direction (primary reinforcement direction) differs from that in the longitudinal direction (distribution reinforcement direction), and a simple method was used to express unit stress in a deck slab.

(6) Deck slabs made of expansive concrete have the effect of reducing the incremental width of cracks caused by drying shrinkage and creep, so that crack width is smaller than in the case of ordinary concrete. This factor may be taken into account when calculating flexural crack at the serviceability limit state.

ACKNOWLEDGEMENT

This study is the results of numerous tests and investigations on the expansive concrete deck slabs at Nagasaki Expressway from 1980 to 1987. For this long term, from the construction work to follow-up study the authors have been received helpfull suggestions and cooperations by many members.

The authors express their deep appreciation to Professor Akira Watanabe and Associate Professor Takashi Idemitsu, Kyushu Institute of Technology, and Professor Yukikazu Tsuji, Gunma University, for their helpful suggestions.

The authors thank members of KODAN, that is, Engineering Department of Head Office, Fukuoka Construction Bureau, Nagasaki Construction Office of Fukuoka Construction Bureau, Experiment Section of Amagi Construction Office of Fukuoka Construction Bureau, Fukuoka Operation Bureau, Isahaya Operation Office of Fukuoka Operation Bureau and Concrete Section of Laboratory for their cooperations. Moreover, the authors thank Cement & Concrete Research Laboratory of Onoda Cement Co., LTD., and Kyushu Saled Office and Bridge Design & Technical Department of Nippon Steel Corporation for their helpful cooperations. And all supporters of this study are gratefully acknowledged.

REFERENCES

[1] JSCE Committee on Investigation of development of Steel Structures : Actuality and trend on Concrete Deck Slabs of Highway Bridges, pp.57～64, February 1985

[2] K. Okada, H. Okamura, K. Sonoda and I. Shimada : Cracking and Fatigue Behavior of Bridge Deck RC Slabs, Proceedings of JSCE, No.321, pp.49～61, May 1982

[3] H. Imai, K. Okada, T. Kojima and Y. Mizumoto : Study of Shrinkage Cracks in Reinforced Concrete Deck Slabs of Bridges, Proceedings of JSCE, No.340, pp.175～184, December 1984

[4] K. Sonoda and T. Horikawa : Low Cycle Fatigue Characteristics of Bridge Deck RC Slabs under the Repetition of wheel Load, Proceedings of JSCE, No.390, pp.97～106, February 1988

[5] S. Matsui and Y. Maeda : A Rational Evaluation Method for Deterioration of Highway Bridge Decks, Proceedings of JSCE, No.374, pp.419～426, October 1986

[6] A. Takeda, T. Endo and N. Fujita : A Consideration on the Mechanism of Detorioration of Bridge Slabs, Transactions of 37th Annual Meeting of Japan Society of Civil Engineers, No.5, pp.9～10, October 1982

[7] Y. Goto and K. Takahashi : Study on the Mechanism of Detorioration of Bridge Slabs and Method for Remedying, Reinforcing and Protecting Them, Report of the Laboratory of Nihon Doro Kodan, the Laboratory of Nihon Doro Kodan, pp.39～56, November 1983

[8] JSCE : Recommended Practice for Expansive Cement Concrete, Concrete Library, No.45, November 1979

[9] Y. Tsuji and H. Okamura : Fundamental Studied on the Improvement of Composite Girders of Steel Beam and Concrete Slab by Using Expansive Concrete, Concrete Journal, JCI, Vol.20, No.2, pp.73～87, February 1982

[10] S. Ohkawa, N. Fujita : An Experiment on RC Slab Decks with Ordinary Concrete and Self-stressing Concrete, 1979 JCI 1st Conference, pp.265～268, May 1979

[11] A. Takeda, S. Nakamura and T. Toyofuku : Consideration on the Crack Control of Steel Bridge Deck Slabs by Using Expansive Concrete, Concrete Journal, Vol.21, No.3, pp.31～39, March 1983

[12] T. Toyofuku, S. Nakamura, K. Jimbo and S. Shirokuni : Study on Early Cracking of Bridge Deck RC Slabs due to Thermal Stress, JCI 7th Conference, pp.13～16, June 1985

[13] T. Toyofuku, K. Sugimoto and S. Irie : Anti-cracking measures of RC Deck Slabs of Steel Bridges by Using Expansive Concrete, 16th Japan Road Conference, Common Section, pp.641～642, October 1985

[14] T. Toyofuku, I. Nishida, and H. Tsurukubo : Crack of Steel Bridge Deck Slabs and That Control by Using Expansive Concrete—Follow-up Study of Nagasaki Expressway's Tarami Bridge—, Concrete Journal, Vol.24, No.2, pp.18～29, February 1986
[15] M. Sakate, F. Machida and Y. Goto : Countermeasures against the crack of Steel Bridge Deck Slab by Using Expansive Concrete, Transactions of 39th Annual Meeting of Japan Society of Civil Engineers, No.5, pp.299～300, October 1984
[16] H. Yoshida, Y. Kawamura and K. Shibata : Anti-cracking measures of Steel Bridge Deck Slabs—Kurinokigawa Bridge in Kanetsu Expressway—, 16th Japan Road Conference, Common Section, pp.639～640, October 1985
[17] S. Sugita, S. Syoya, T. Suzuki and T. Miyazaki : A Consideration on Improvement of Durability of Steel Bridge Deck Slab by Using Expansive Concrete, Transactions of 41th Annual Meeting of Japan Society of Civil Engineers, No.1, pp.477～478, November 1986
[18] NIHON DORO KODAN (Japan Highway Public Corporation) : Manual for Maintenance and Repair (Deck Slabs of Bridges), July 1978
[19] K. Shiina : Humidity and Deformation of Concrete, Concrete Journal, Vol.7, No.6, pp.1～11, June 1969
[20] M. Shoya and H. Tokuda : Study on the Moisture Loss and Drying Shrinkage of Concrete due to Wind Action, Preceedings of JSCE, No.328, pp.121～134, December 1982
[21] S. Iwama : Experimental Studies on the Structural Design of Concrete Pavement, Proceedings of JSCE, No.111, pp.16～46, November 1964
[22] The Committee Report : Identification of Degree of External Restraint and the Proposed Method of Thermal Stress Calculation of Massive Concrete Reported by JCI Committee on Thermal Stress of Massive Concrete, Concrete Journal, Vol.23, No.8, pp.4～14, August 1985
[23] Japan Concrete Institute : Recommendations for Control of Cracking in Massive Concrete, March 1986
[24] Japan Road Association : Specifications for Highway Bridges and its Comments, February 1973
[25] Japan Society of Civil Engineers : Standard Specification for Design and Construction of Concrete Structures, Part 2 (Design), October, 1986
[26] Japan Society of Civil Engineers : Rivision Data of Standard Specification for Design and Construction of Concrete Structures (1986), Concrete Library, No.61, pp.196～228, October 1986
[27] Y. Kakuta : Maximum Crack Widths in Reinforced Concrete, Concrete Journal, Vol.8, No.9, pp.1～10, September 1970
[28] Y. Ozaka, K. Ohtsuka and Y. Matsumoto : Crack formed in Concrete Prism with Axial Tension Bars under Influence of Drying, Concrete Journal, Vol.23, No.3, pp.109～119, March 1985